

# Controlled manipulation of light by cooperative response of atoms in an optical lattice

Stewart D. Jenkins and Janne Ruostekoski

*School of Mathematics, University of Southampton, Southampton SO17 1BJ, United Kingdom*

(Dated: October 31, 2018)

We show that a cooperative atom response in an optical lattice to resonant incident light can be employed for precise control and manipulation of light on a subwavelength scale. Specific collective excitation modes of the system that result from strong light-mediated dipole-dipole interactions can be addressed by tailoring the spatial phase-profile of the incident light. We demonstrate how the collective response can be used to produce optical excitations at well-isolated sites on the lattice.

PACS numbers: 03.75.Lm, 32.80.Qk

Accurate control of ultracold atomic gases in periodic optical lattices, in which interactions are well understood, opens the door to unique and intriguing opportunities to study many-particle phenomena and their applications. Experimental progress has led to observations of novel strongly-interacting states, e.g., in quantum phase transitions [1–5] and fermionic pair condensation [6]. Many-body quantum entanglement has been generated via controlled atom collisions [7], lattice systems have been used for preparation of spin-squeezed states for sub-shot-noise interferometry [8], and the atoms can now even be manipulated in a single-spin level at a specific lattice site [9]. On the other hand, recent developments in nanofabrication of arrays of circuit elements acting as plasmonic resonators has stimulated interest in photonic metamaterials. A metamaterial is an artificially tailored crystal consisting of subwavelength-scale structures that can manipulate light on a nanoscale. Here we show that a basic Mott-insulator state of a neutral gas of ultracold atoms confined in an optical lattice, or artificial light crystal, exhibits strongly interacting electric dipole transitions leading to a cooperative response. Such collective behavior can influence resonant imaging and may also be employed to form a metamaterial for precise control and manipulation of optical fields on a subwavelength scale, providing an interesting nanophotonic tool.

In this letter, we consider an ultracold gas of atoms confined in a two-dimensional (2D) optical lattice with precisely one atom per site. Such a system can be prepared, e.g., in a weak harmonic trap or by engineering a Mott-insulator state of atoms by single-site addressing of atomic spins [9]. Resonant, coherent light whose spatial phase-profile is adjusted, e.g., by a hologram or spacial light modulator, illuminates the lattice. The scattered light mediates strong many-particle dipole-dipole (DD) interactions between atoms, leading to a cooperative atom response. The optical excitations of the atoms exhibit collective modes with resonance frequencies and radiative linewidths that dramatically differ from those of an isolated atom. We demonstrate the idea of subwavelength-scale light manipulation by engineering the spatial phase-profile of an incident monochromatic plane-wave. The tailored incident field produces localized dipolar subwavelength-scale excitations of the atoms in desired locations in the lattice. By dynamically

adjusting the phase pattern of the field, the excitations can be controlled and moved around in the lattice.

The particular example of subwavelength-scale localization of optical excitations we study here has attracted considerable interest in nanophotonics with possibilities for microscopy and data storage applications. Spatial and temporal modulation of ultrashort laser pulses leads to excitation of energy hot-spots in nanostructures [10, 11]. It has also been proposed that interactions between induced currents and plasmonic waves on nanostructures permits the excitation of subwavelength hot-spots by amplitude or phase modulated monochromatic fields [12, 13].

Non-trivial collective optical properties result from a cooperative response of the strongly interacting, closely-spaced atoms: recurrent scattering events, in which a photon is repeatedly scattered by the same atom, lead to collective modes with strongly modified spatial configurations and radiation rates [14–17]. Such scattering processes can result in light localization that is analogous to Anderson localization of electrons [18]. The resonant response is very different from the studies of off-resonant optical diagnostics of atomic correlations in optical lattices [19–25]. Photonic band gaps for atomic lattices have previously been calculated in Ref. [26].

For our lattice system we numerically calculate the optical response by stochastically sampling the atomic positions according to their spatial distributions then solving the recurrent scattering events to all orders for each stochastic realization. We find a strong resonant response in the case of closely-spaced atoms with the near-field emission pattern from the atoms forming sharp, narrow spatially localized amplitude peaks. The response is sensitive to detuning of the incident light from the atomic resonance and to the spatial separation between the atoms. Tuning light off-resonant or increasing the lattice spacing rapidly leads to suppressed interactions. If the atoms are not confined strongly enough to the individual lattice sites, the resulting increased disorder in the atomic positions due to quantum fluctuations also suppresses the strong collective effects in the ensemble-averaged response.

We take the atoms to occupy the lowest energy band in a 2D square optical lattice of periodicity  $a$  in the  $xy$  plane as described in Appendix A. We assume that the atoms

are tightly confined to the lowest vibrational state in the  $z$  direction of an oblate external potential and that they reside in the Mott-insulator state with precisely one atom per site. In a combined harmonic trap and the lattice the single-occupancy state of bosonic atoms can exist in a weak harmonic trap or can be engineered from the typical ‘wedding-cake’ Mott-insulator ground state by manipulating the multi-occupancy states, e.g., by single-site addressing or by inducing atom parity-dependent losses [9]. In a deep lattice, the vibrational ground-state wavefunction (the Wannier function) is approximately that of a harmonic oscillator with frequency  $\omega = 2\sqrt{s}E_R/\hbar$  where  $s$  denotes the lattice depth in the units of the lattice-photon recoil energy  $E_R = \pi^2\hbar^2/(2ma^2)$  [27]. The confinement of the atoms along the lattice in the  $xy$  plane in each site  $j$  thus has a Gaussian density profile,  $\rho_j(\mathbf{r})$ , with the  $1/e$  width  $\ell = as^{-1/4}/\pi$  controlled by the lattice depth  $s$  and the lattice spacing  $a$ .

We illuminate the lattice with a monochromatic incident field  $\mathbf{E}_{\text{in}}(\mathbf{r}, t)$  whose frequency  $\Omega$  is nearly resonant on an electric dipole transition. This impinging field excites the dipole transition of the atoms, producing scattered light that, in turn, impact the driving of neighboring atoms and alter their scattered light. The scattered photons can mediate strong interactions between closely-spaced atoms, so that the atomic system responds to light cooperatively, exhibiting *collective* excitation eigenmodes. Here, we show how to exploit these interactions for controlling and manipulating light on a subwavelength scale. As a specific example, we prepare subwavelength-scale spatially localized collective excitations of the atoms in isolated regions of the lattice by considering an incident plane-wave illumination of the atoms with an approximately sinusoidal phase-profile. Such a response is distinct from that which would be seen if the atoms did not interact.

In order to model the cooperative atom response to light, we assume the incident field is sufficiently weak that saturation of the excited state can be neglected. For simplicity, we consider the atomic internal states as an effective two-level system consisting of a single electronic ground and excited state. On impact, light drives atomic transitions inducing a polarization density  $\mathbf{P}^+(\mathbf{r}, t) = \sum_j \mathbf{P}_j^+(\mathbf{r}, t)$ , where the polarization within each site  $j$ ,  $\mathbf{P}_j^+(\mathbf{r}, t) = \mathbf{d}_j \delta(\mathbf{r} - \mathbf{r}_j)$  and  $\mathbf{d}_j$  is the electric dipole moment of an atom at site  $j$ . To facilitate numerical evaluation of the lattice response, we express the polarization in terms of stochastic amplitudes  $e_j$ , representing the coherence of atoms  $j$  realized for a stochastic sampling of atomic positions from the atomic density distributions  $\rho_j(\mathbf{r}_j)$ , such that  $\mathbf{P}_j^+(\mathbf{r}, t) = e^{-i\Omega t} \wp \hat{\mathbf{d}} \delta(\mathbf{r} - \mathbf{r}_j) e_j(t)$ , where  $\wp$  is the atomic dipole matrix element. When the atomic dynamics evolve on timescales much longer than the light propagation time across the optical lattice [16], the induced polarization produces the scattered electric displacement field  $\mathbf{D}_{S,j}^+(\mathbf{r}) = k^3/(4\pi) \int d^3r' \mathbf{G}(\mathbf{r} - \mathbf{r}') \cdot \mathbf{P}_j^+(\mathbf{r}')$ , where  $\mathbf{G}(\mathbf{r} - \mathbf{r}')$  is the monochromatic dipole radiation kernel representing the radiated field at  $\mathbf{r}$  from a dipole

residing at  $\mathbf{r}'$  [28]. Thus, the atom at site  $j$  experiences driving by the sum of fields  $\mathbf{D}_{S,j'}$  scattered from all other atoms in the lattice and the incident field  $\mathbf{D}_{\text{in}}$ ; these scattered fields are proportional to the amplitudes  $e_{j'}$  of their atoms of origin. These multiple scattering processes therefore produce collective dynamics described by

$$\dot{e}_j = (i\delta - \Gamma/2)e_j + \sum_{j' \neq j} \mathcal{C}_{j,j'} e_{j'} + F_j, \quad (1)$$

$$\mathcal{C}_{j,j'} \equiv \frac{3\Gamma}{2i} \hat{\mathbf{d}} \cdot \mathbf{G}(\mathbf{r}_j - \mathbf{r}_{j'}) \cdot \hat{\mathbf{d}}, \quad (2)$$

where  $F_j \equiv e^{i\Omega t} \wp \hat{\mathbf{d}} \cdot \mathbf{D}_{\text{in}}^+(\mathbf{r}_j)/(i\hbar\epsilon_0)$  is the direct driving of the atom in site  $j$  by the incident field,  $\delta \equiv \Omega - \omega_{e,g}$  is the detuning of the field from resonance, and  $\Gamma$  is the spontaneous emission rate. For each stochastic realization of atomic positions, interactions between  $N$  atoms in an optical lattice lead to the formation of  $N$  *collective* atomic excitations, each with its own resonance frequency and spontaneous emission rate, which could have either super-radiant or sub-radiant characteristics.

By exploiting the strong DD interactions, one can tailor the incident field so that it excites specific linear combinations of collective modes, providing a desired response. Here, for example, we consider a linearly-polarized ( $\hat{\mathbf{e}}_y$  chosen to be parallel to the lattice plane), phase-modulated field whose positive frequency component reads

$$\mathbf{E}_{\text{in}}^+(\mathbf{r}, t) \simeq \hat{\mathbf{e}}_y E_0 e^{i\varphi(x,y)} e^{i(kz - \Omega t)}, \quad (3a)$$

$$\varphi(x, y) = \frac{\pi}{2} \sin(\kappa x) \sin(\kappa y). \quad (3b)$$

A field profile of this form, however, contains evanescent plane-wave components whose transverse wavevectors exceed the carrier wave number  $k = 2\pi/\lambda = \Omega/c$ . We therefore approximate it through the truncated Fourier expansion as described in Appendix C. One can produce such a field, e.g., by a hologram or a spatial light modulator. Figure 1 illustrates how the field Eq. (3) can excite a checkerboard pattern of localized excitations of atoms in a lattice. In these calculations, we neglect the width of the atomic wavefunctions in the  $z$  direction, as a width on the order of  $\ell$  in the  $z$  direction has a negligible effect on the calculated response. We fully incorporate, however, quantum fluctuations of the atomic positions on the lattice plane in the vibrational ground state of each site. The many-atom correlations of the specific one-atom Mott-state are also included. As we discuss below, interactions between the atoms are vital to the realization of this pattern. The atoms are arranged in an  $18 \times 18$  square lattice with the spacing  $a = 0.55\lambda$ , and a site residing at  $(x_0, y_0) = (a/2, a/2)$ . The incident field [Eq. (3)] has a modulation period  $2\pi/\kappa = 6a$ , indicating the periodicity of  $\mathbf{E}_{\text{in}}(\mathbf{r}, t)$  of six sites. We choose the dipole orientation  $\hat{\mathbf{d}} \approx \hat{\mathbf{e}}_z + 0.1\hat{\mathbf{e}}_y$  to be slightly rotated from the normal to the lattice plane so that the atoms scatter fields largely within the plane while allowing them to be driven by the incident field. The collective mode

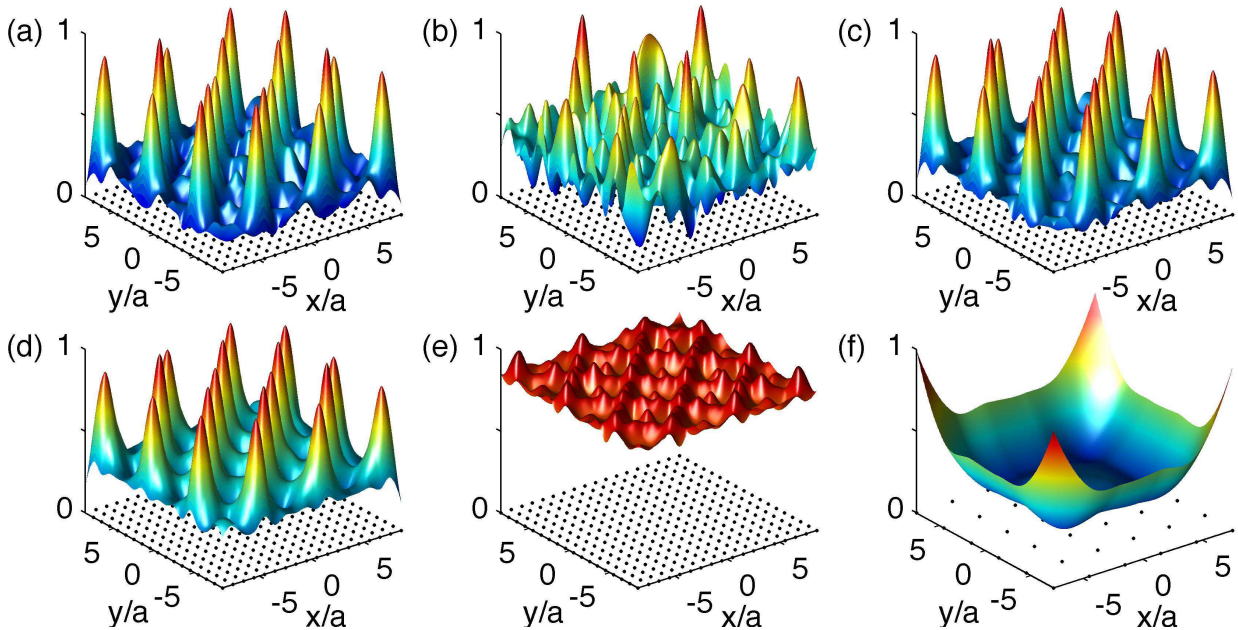


FIG. 1: The atomic excitation intensities  $\overline{|e_j|^2 / \max_{j'} |e_{j'}|^2}$  resulting from the cooperative response of an ensemble of two-level atoms in an optical lattice to a phase modulated incident field [Eq. (3)] with modulation period of 6 lattice sites. The black dots indicate the positions of the populated lattice sites. In panel (a), the atoms are perfectly confined at the center of each site and their wavefunctions have width  $\ell = 0$ . Panel (b) represents the response of a single stochastic realization of atomic positions sampled from a 2D Gaussian variables of width  $0.12a$  centered on the lattice sites. Panels (c), (e-f) the show responses of atoms whose wavefunction widths  $\ell = 0.12a$  calculated from an ensemble average over several thousand realizations of atomic positions, while in panel (d)  $\ell = 0.21a$ . In panel (e), the incident field is detuned from the resonance of an isolated atom by  $10\Gamma$ , while the detuning is zero for all other panels. In panel (f), atoms were removed from 8/9 of the sites, thus removing the role of the other sites from the cooperative response and destroying the pattern observed in panels (a) and (c).

spontaneous emission rates range from a very subradiant  $3 \times 10^{-3}\Gamma$  to the superradiant  $5\Gamma$ , while their frequency shifts from the single atom resonance range from  $-2\Gamma$  to  $0.9\Gamma$ .

We first consider an infinitely deep lattice in which the atoms are perfectly confined at the center in their respective sites, i.e., with  $\ell = 0$ . In this case, the atomic positions are deterministic and Eq. (1) reduces to a coupled set of linear equations whose steady-state solutions for  $|e_j|^2$  are shown in Fig. 1a. A subset of atoms residing at the local minima of  $\varphi(x, y)$  are more strongly excited than those in the surrounding lattice sites, while those at the local maxima of  $\varphi(x, y)$  are roughly as weakly excited as their surroundings. The peaks sit on a background with excitations roughly 0.2 times those of the most excited atoms. We find a subwavelength excitation FWHM width of the peak to be less than  $0.9\lambda$ . This results in a checkerboard pattern with the localized excitations separated by  $3\sqrt{2}$  sites (3 sites in the both directions) sitting on a background of weakly excited atoms. The regularity of the response can be broken by slightly altering the period or the orientation of the phase modulation. Note that the periodicity of the incident field is significantly larger than the width of the localized excitations.

In a more realistic scenario, the width of the lattice site atomic wavefunction due to vacuum fluctuations cannot be neglected and the scattered light sources are essentially distributed over the atomic densities. To obtain the average atomic excitations  $\overline{|e_j|^2}$  that dominate the near-field emission, we solve Eq. (1) through Monte-Carlo integration [29]. We obtain a large number of realizations of atomic positions  $\mathbf{r}_j$  in each site  $j$  sampled from a probability distribution matching the single-atom density function. Then for each realization, we solve Eq. (1) as if the atoms were localized at the sample points. We then compute  $|e_j|^2$  for each sample, and perform an ensemble average over all realizations of atomic positions. Each stochastic realization represents a possible outcome of a single experimental run in which case atomic positions are localized due to the measurement of scattered photons.

Quantum fluctuations of atomic positions in individual sites can dramatically affect the response. We demonstrate this showing in Fig. 1b the excitation intensities for a single stochastic realization of atomic positions in which case a single atom in each site is independently sampled from the Gaussian density-distribution of width  $\ell = 0.12a$  (corresponding to the lattice height  $s \simeq 50$ ).

The non-regularity of the lattice alters the collective modes for the sample realization. Although the atoms are driven by the same incident field that gives rise to the pattern in Fig. 1a, the displacement drastically alters the collective interaction, and yields an optical response with a significant stochastic noise and a less regular array of localized peaks. Such effects can be washed out when one calculates the ensemble average of the response that corresponds to expectation values obtained over many experimental realizations. The excitation intensity  $\overline{|e_j|^2}$  averaged over 6400 position realizations for Wannier functions of width  $\ell = 0.12a$  is shown in Fig. 1c for the same parameters as those in Fig. 1a. With atomic wavefunction of this width, the collective interactions producing the pattern of Fig. 1a survive the averaging process, providing an excitation with subwavelength FWHM and a background excitation comparable to that calculated for perfectly localized atoms in an infinitely deep lattice. Weaker confinement only moderately diminishes the cooperative interactions. For  $\ell = 0.21a$ , corresponding to  $s \simeq 5$ , Fig. 1d shows a weakening contrast of the pattern with a background excitation approximately 0.3 times that of the peaks, which themselves have slightly broader FWHM of  $1.2\lambda$ .

We can illustrate the essential nature of cooperative interactions in the formation of this excitation pattern by suppressing the DD interactions and observing the result. Fig. 1e shows the response of the atoms in the optical lattice of Fig. 1c to an incident field detuned from the single atom resonance by  $10\Gamma$ . Since, with this detuning, each photon interacts more weakly with an individual atom, the probability of a multiple scattering process for a two-level atom reduces geometrically with the number of single scattering events involved in that process [17]. The interactions resulting from these multiple scattering events are therefore suppressed. While the incident field has the same phase modulation as in Figs. 1a-d, the excitation pattern is not preserved. Atoms at sites where the phase modulation  $\varphi$  is minimized are not appreciably more excited than the surrounding background as in Figs. 1a and c.

The pattern formation in Figs. 1a,c truly represents a cooperative response where the interactions between all the atoms in the lattice, including also the weakly excited ones, are essential. We illustrate this in Fig. 1f, where all of the atoms not residing at the maxima or minima of the incident field phase modulation  $\varphi$  have been removed from the lattice. In effect, the lattice spacing was tripled to  $a' = 3a = 1.65\lambda$ , with an atom residing at  $(x_0, y_0) = (a'/2, a'/2)$ . If the removed atoms had not played an essential role, the response of the lattice would show a checkerboard pattern of strongly excited and weakly excited atoms. However, the system response displayed in Fig. 1f shows that the atoms in the interior of the lattice are excited roughly evenly even though each atom is driven with an opposite phase to that of its nearest neighbor. Atoms at the edge of the sample are more strongly excited due to finite size effects.

Sharp localized excitations may be broadened by heating and losses that can inhibit the cooperative atom response. Raman transitions to other vibrational center-of-mass states heat up the atoms, broadening the atomic density distributions in individual sites and increasing the hopping amplitude of the atoms between the adjacent sites. Such processes could be reduced, e.g., due to the orthogonality of the eigenfunctions in each site, if the electronic ground and excited state atoms approximately experience the same lattice potential even if the system is not in the Lamb-Dicke regime. Alternatively, if the atomic linewidth is much larger than the trapping frequency, the collective response may reach a steady state before the heating becomes deleterious. Additional atom losses due to Raman transitions to other internal states could be avoided if each atom forms an effective two-level system of a single electronic ground and excited state. A desired two-level configuration could be realized with a cycling transition by shifting all other transitions out of resonance or with a  $J = 0 \rightarrow J = 1$  transition with all except one excited state shifted out of resonance.

In conclusion, we have shown that resonant DD interactions between atoms in an optical lattice lead to a collective response that can be exploited in manipulation of light on a subwavelength scale. To illustrate this, we studied an example of engineering a checkerboard pattern of isolated atomic excitations. Unlike in nanofabricated metamaterial samples [10–13], here the effect is not based on interactions between plasmonic and current excitations but purely electric DD interactions between neutral atoms without magnetic contributions. Moreover, the positions of the excitations can be dynamically altered simply by translating the phase-modulation pattern, so that the collective excitation pattern adiabatically follows the change in the phase pattern. By understanding these interactions, the characteristics of an incident field could be engineered to produce more complex excitations. Our example also demonstrates how a cooperative response can have implications on the resonant absorption imaging of 2D atomic samples in which case deviations from the column density results have been experimentally observed [30]. Moreover, the non-trivial relationship between incident field modes and the collective excitations to which they couple could be of importance, e.g., to imaging and to the implementation of quantum memories in optical lattice systems in which the states of a light field are mapped onto collective hyperfine excitations in the lattice.

## Acknowledgments

We acknowledge financial support from the Leverhulme Trust and the EPSRC.



## Appendix

In these appendices, we provide some of the technical details of the optical lattice system and the incident field used to excite it. In Appendix A, we describe the optical lattice potential. In Appendix B, we describe the dynamics of the atomic dipoles interacting with both the incident and scattered electric fields. Finally in Appendix C, we describe how one can construct the approximate phase modulated driving field used to illuminate the optical lattice system and excite collective atomic excitations that were discussed in the text.

### Appendix A: The Optical Lattice Trapping Potential

We consider a two-dimensional square optical lattice of periodicity  $a$ , centered on the point  $(x_0, y_0, 0)$ . Four intersecting beams produce the optical confining potential

$$V = sE_R \left[ \sin^2 \left( \pi \frac{x - x_0}{a} \right) + \sin^2 \left( \pi \frac{y - y_0}{a} \right) \right] \quad (\text{A1})$$

where  $E_R = \pi^2 \hbar^2 / (2ma^2)$  is the lattice recoil energy [27], and the dimensionless confinement strength  $s$  controls the width of the vibrational ground-state wavefunction in each site (Wannier functions) that results from single-particle quantum fluctuations. An additional potential tightly confines the atoms in the  $z = 0$  plane. The lattice resides in a Mott-insulator state with precisely one atom per lattice site. Each lattice site, labeled by index  $j$ , has a potential minimum located at position  $\mathbf{R}_j$ , and the Wannier function  $\phi_j(\mathbf{r}) \equiv \phi(\mathbf{r} - \mathbf{R}_j)$ . When the confinement is sufficiently tight, the potential  $V$  in the neighborhood of each lattice site is roughly harmonic with

$$V(\mathbf{r}) \approx \frac{m}{2} \sum_{\mu=x,y,z} \omega_\mu^2 (\Delta r_\mu)^2 \quad (\text{A2})$$

where  $\omega_x = \omega_y = 2\sqrt{s}E_R/\hbar$ ,  $\omega_z$  is the trapping frequency along the  $z$  direction, and  $\Delta r_\mu \equiv \hat{\mathbf{e}}_\mu \cdot (\mathbf{r} - \mathbf{R}_j)$  is the displacement of the  $\mu$ th component of  $\mathbf{r}$  from the lattice site  $\mathbf{R}_j$ . An atom in each site occupies the ground state of the harmonic oscillator potential

$$\phi(\mathbf{r}) = \frac{1}{(\pi^3 \ell^4 \ell_z^2)^{1/4}} \exp \left( -\frac{x^2 + y^2}{2\ell^2} - \frac{z^2}{2\ell_z^2} \right), \quad (\text{A3})$$

where the width of the of the wave function is  $\ell = as^{-1/4}/\pi$ , and its thickness  $\ell_z = \sqrt{\hbar/(m\omega_z)}$ . The atomic density,  $\rho_j(\mathbf{r}) \equiv |\phi_j(\mathbf{r})|^2$ , at site  $j$  thus has a Gaussian profile with a  $1/e$  radius  $\ell$  in the  $xy$  plane. This width is directly proportional to the lattice spacing and narrows with increased trapping strength  $s$ . It is possible to adjust the lattice spacing by using accordion lattices [31]. Moreover, the relationship between the lattice spacing and the Wannier wavefunction confinement may be controlled by magnetic field dressing [32].

## Appendix B: Dynamics of atomic excitations in the lattice

In this section, we elaborate on the dynamics of the atomic electric dipoles interacting with light. We show that the evolution of the system can be described as in Eq. (2) of the main text. We then discuss the Monte-Carlo method used to compute the average excitation energies  $\overline{|e_j|^2}$  displayed in Fig. 1 of the text.

### 1. Basic model

We consider an ensemble  $N$  two-level atoms placed in harmonic potentials centered at the lattice sites  $\mathbf{R}_j$  ( $j = 1, \dots, N$ ). Each atom has an internal ground state  $|g\rangle$  and an excited state  $|e\rangle$  which differ in energy by  $\hbar\omega_{e,g}$ . A coherent, monochromatic field  $\mathbf{D}_{\text{in}}^+(\mathbf{r}, t)$  with frequency  $\Omega$  impinges on the lattice. The field incident on the atoms in the lattice drives the  $|g\rangle \leftrightarrow |e\rangle$  transition, inducing a polarization density  $\mathbf{P}^+(\mathbf{r}, t) = \sum_j \mathbf{P}_j^+(\mathbf{r}, t)$ , where the polarization due to an atom in site  $j$ ,  $\mathbf{P}_j^+ = \mathbf{d}_j \delta(\mathbf{r} - \mathbf{r}_j)$ ,  $\mathbf{d}_j$  is the dipole moment of an atom in site  $j$ , and  $\mathbf{r}_j$  is its position coordinate. Scattering of light from the atoms produces correlations between the positions of the atoms and the scattered field profile. In this way, continuous measurement of the scattered light yields an effective measurement of the atomic positions. This process simultaneously projects the position coordinates of an atom in each site  $j$  onto a specific position  $\mathbf{r}_j$  through the projection operator  $\hat{Q}(\{\mathbf{r}_j\}) \equiv \bigotimes_{j=1}^N |\mathbf{r}_j\rangle_j \langle \mathbf{r}_j|$  acting on the initial vibrational state of the system, where  $\{\mathbf{r}_j\}$  denotes the set  $\{\mathbf{r}_1, \dots, \mathbf{r}_N\}$  of realized position coordinates for atoms in lattice sites  $\{1, \dots, N\}$ . We therefore characterize the evolution of the polarization density associated with site  $j$  in terms of the slowly varying coherence conditioned on the realized atomic position  $\mathbf{r}_j$ , and the positions in all other sites  $\mathbf{r}_{j'}$  for  $j' \neq j$ . We define the amplitudes  $e_j(\mathbf{r}_j, t; \{\mathbf{r}_{j' \neq j}\}) \equiv e^{i\Omega t} \langle \sigma_j \rangle_{\{\mathbf{r}_1, \mathbf{r}_2, \dots, \mathbf{r}_N\}}$  to be the slowly varying coherence between the ground and excited states of an atom at site  $j$  conditioned on the observation of atoms at positions  $\{\mathbf{r}_1, \mathbf{r}_2, \dots, \mathbf{r}_N\}$  within their respective sites, where  $\sigma_j$  is the coherence operator for an atom in site  $j$ . For a single realization of position coordinates of the atoms, the polarization in site  $j$  depends on the position of all the atoms via the amplitudes  $e_j$ :

$$\mathbf{P}_j(\mathbf{r}, t; \{\mathbf{r}_{j'}\}) = e^{-i\Omega t} \hat{\mathbf{d}}_\varphi \delta(\mathbf{r} - \mathbf{r}_j) e_j(\mathbf{r}_j, t; \{\mathbf{r}_{j' \neq j}\}), \quad (\text{B1})$$

where  $\varphi$  is the dipole matrix element. In addition to the incident electric field, an atom at site  $j$  experiences driving by the fields  $\mathbf{D}_{S,j'}^+$  scattered from all other sites  $j' \neq j$  in the lattice. The total displacement field arriving at this site is thus

$$\mathbf{D}_{\text{ext},j}^+(\mathbf{r}, t) \equiv \mathbf{D}_{\text{in}}^+(\mathbf{r}, t) + \sum_{j' \neq j} \mathbf{D}_{S,j'}^+(\mathbf{r}, t). \quad (\text{B2})$$

When the atomic dynamics evolve on timescales much longer than the time it takes for light to propagate across the optical lattice, the scattered fields can be expressed in the monochromatic limit as [16, 17]

$$\mathbf{D}_{S,j}^+(\mathbf{r}) = \frac{k^3}{4\pi} \int d^3r' \mathbf{G}(\mathbf{r} - \mathbf{r}') \cdot \mathbf{P}_j^+(\mathbf{r}'), \quad (\text{B3})$$

where  $k = \Omega/c$ , and  $\mathbf{G}$  is the radiation kernel with tensor components

$$\mathbf{G}_{\mu,\nu}(\mathbf{r}) = \frac{1}{k^2} (\partial_\mu \partial_\nu - \delta_{\mu,\nu} \nabla^2) \frac{e^{ikr}}{kr}. \quad (\text{B4})$$

The monochromatic dipole radiation kernel, representing the radiated field at  $\mathbf{r}$  from a dipole residing at  $\mathbf{r}'$ , can be expressed as [28]

$$\mathbf{G}(\mathbf{r}) = \left[ \frac{2}{3} + \left( \frac{\mathbf{r}\mathbf{r}}{r^2} - \frac{1}{3} \right) \left( \frac{3 - 3ikr - k^2r^2}{k^2r^2} \right) \right] \frac{e^{ikr}}{kr} + \frac{8\pi}{3} \delta(kr). \quad (\text{B5})$$

## 2. Stochastic simulations

In the simulations we solve the cooperative optical response of the atomic sample to the incident field using a Monte-Carlo approach in which the position coordinates of the atoms are sampled according to their position correlation functions, and the optical response is calculated for each stochastic realization [29]. We assume that the atoms form a Mott-insulator state of precisely one atom per lattice site. The position coordinates of atoms within each site  $j$  are therefore independent stochastic variables, sampled from Gaussian distributions  $\rho_j(\mathbf{r})$ . The atoms reside at the vibrational ground states of the lattice sites and the Gaussian distribution  $\rho_j(\mathbf{r})$  results from the single-particle quantum fluctuations, determined by the Wannier wavefunction density in the particular site  $j$ . The atomic position in the site  $j$  is centered at  $\mathbf{R}_j$ . The width of the Wannier wavefunction is determined by the lattice confinement. Since each stochastic realization of position coordinates for the atoms in the  $N$  lattice sites  $\{\mathbf{r}_1, \mathbf{r}_2, \dots, \mathbf{r}_N\}$  can be interpreted as an outcome of a continuous measurement process of scattered light that localizes the atoms, each stochastic Monte-Carlo trajectory also represents a possible outcome of a single experimental run. We evaluate the ensemble averages of the atomic optical excitations by computing the excitations for each of many stochastic realizations of position coordinates of the atoms and then calculating their ensemble average. The numerically calculated ensemble average then corresponds to the experimentally measured ensemble average over many experimental runs and provides quantum mechanical expectation values of the observables.

In order to calculate the optical response for each stochastic realization of position coordinates for the

atoms in the  $N$  lattice sites,  $\{\mathbf{r}_1, \mathbf{r}_2, \dots, \mathbf{r}_N\}$ , we assume here that the incident light is sufficiently weak that we can neglect the excited state saturation of the atoms. In this limit, the coherence amplitude for an atom in site  $j$  obeys the equations of motion

$$\frac{d}{dt} e_j = (i\delta - \Gamma/2) e_j + e^{i\Omega t} \frac{\mathcal{S}}{i\hbar\epsilon_0} \hat{\mathbf{d}} \cdot \mathbf{D}_{\text{ext},j}^+(\mathbf{r}_j, t), \quad (\text{B6})$$

where  $\delta \equiv \Omega - \omega_{e,g}$  is the detuning of the incident light from the resonance of the atomic transition and  $\Gamma$  is the atomic spontaneous emission rate. For each stochastic realization of atomic positions, the light impinging on an atom in a particular site consists of the incident field and the scattered light from all the other  $N - 1$  sites. Because light scattered from an atom is directly proportional to its coherence amplitude, we obtain

$$\frac{d}{dt} e_j = (i\delta - \Gamma/2) e_j + \sum_{j' \neq j} \mathcal{C}_{j,j'} e_{j'} + e^{i\Omega t} \frac{\mathcal{S}}{i\hbar\epsilon_0} \hat{\mathbf{d}} \cdot \mathbf{D}_{\text{in}}^+(\mathbf{r}_j, t), \quad (\text{B7})$$

where  $\mathcal{C}_{j,j'}$  is the coupling matrix element representing the effect of dipole radiation from the atom in site  $j'$  on the coherence amplitude of the atom in site  $j$ ;

$$\mathcal{C}_{j,j'} = \frac{3\Gamma}{2i} \hat{\mathbf{d}} \cdot \mathbf{G}(\mathbf{r}_j - \mathbf{r}_{j'}) \cdot \hat{\mathbf{d}}. \quad (\text{B8})$$

For each stochastic realization of position coordinates of the atoms, Eq. (B7) represents a collective response of the atomic sample to the incident light. Repeated exchanges of a photon between the same atoms lead to cooperative response of the atoms. The system exhibits collective eigenmodes with each eigenmode associated with a specific resonance frequency and a radiative linewidth. In the text, we considered an  $18 \times 18$  array with lattice spacing  $0.55\lambda$  ( $\lambda = 2\pi c/\Omega$ ), and dipole orientations  $\hat{\mathbf{d}} \approx \hat{\mathbf{e}}_z + 0.1\hat{\mathbf{e}}_y$ . For this configuration, when the atoms are placed precisely at the centers of the lattice sites  $\mathbf{R}_j$ , the collective mode spontaneous emission rates range from a very subradiant  $3 \times 10^{-3}\Gamma$  to the superradiant  $5\Gamma$ , while their collective frequency shifts from the single atom resonance range from  $-2\Gamma$  to  $0.9\Gamma$ .

In each stochastic realization of position coordinates of atoms within their respective lattice sites, we solve the steady-state solution of the excitation amplitudes of the atom in each lattice site  $e_j$  by setting  $de_j/dt = 0$  in Eq. (B7). The results for a single stochastic realization of  $|e_j|^2$  are displayed in the main text. We then compute the ensemble average of the atomic excitation  $\overline{|e_j|^2}$  by averaging over a sufficiently large number of stochastic realizations. That is, we take  $\mathcal{N}$  stochastic realizations of the position coordinate of an atom within each site  $j$ . For the  $\nu$ th realization ( $\nu = 1, \dots, \mathcal{N}$ ) we have sampled the position coordinates of an atom in site  $j$ ,  $\mathbf{r}_j^{(\nu)}$ . For these atomic positions, we solve the steady state of Eq. (B7) to obtain the atomic amplitudes  $e_j^{(\nu)}$  and calculate the

ensemble average

$$\overline{|e_j|^2} = \frac{1}{N} \sum_{\nu=1}^N \left| e_j^{(\nu)} \left( \mathbf{r}_j^{(\nu)}; \{ \mathbf{r}_{j' \neq j}^{(\nu)} \} \right) \right|^2. \quad (\text{B9})$$

### 3. Many-particle correlations

In this paper we consider a specific many-particle atom state: the bosonic Mott-insulator state with precisely one atom per site. The atoms reside in the lowest vibrational state of each lattice site. Vacuum fluctuations for the position of the single-particle state of the atoms are incorporated in the Monte-Carlo sampling of the atomic positions from the Gaussian density distribution, determined by the Wannier wavefunctions of each lattice site. As we will show below, for the specific Mott-state of one atom per site, the sampling procedure also represents all the many-particle correlations of the system.

The joint probability distribution  $P(\bar{\mathbf{r}}_1, \dots, \bar{\mathbf{r}}_N)$  for the positions of the  $N$  atoms is given by the absolute square of the normalized many-particle wavefunction

$$P(\bar{\mathbf{r}}_1, \dots, \bar{\mathbf{r}}_N) = |\Psi(\bar{\mathbf{r}}_1, \dots, \bar{\mathbf{r}}_N)|^2 \quad (\text{B10})$$

$$P(\bar{\mathbf{r}}_1, \dots, \bar{\mathbf{r}}_N) \simeq \frac{1}{N!} \sum_{j_1 \dots j_N} |\phi_{j_1}(\bar{\mathbf{r}}_1)|^2 \dots |\phi_{j_N}(\bar{\mathbf{r}}_N)|^2 \quad (\text{B11})$$

Here the coordinates of the  $N$  atoms are denoted by  $(\bar{\mathbf{r}}_1, \dots, \bar{\mathbf{r}}_N)$ . The summation runs over all possible  $N$ -tuples  $(j_1, \dots, j_N)$  of the state labels  $j = (1, \dots, N)$  referring to the lattice sites  $j$  with precisely one atom per site. The Wannier wavefunctions for each lattice site  $\phi_j$  in Eq. (B11) are assumed to have a negligible overlap with the neighboring sites, so that  $\phi_j(\mathbf{r})\phi_k(\mathbf{r}) \simeq 0$ , whenever  $j \neq k$ . Since we have exactly one atom per site, we may rewrite the joint probability distribution of Eq. (B11) as

$$P(\bar{\mathbf{r}}_1, \dots, \bar{\mathbf{r}}_N) \simeq \frac{1}{N!} \sum_{i_1 \dots i_N} |\phi_1(\bar{\mathbf{r}}_{i_1})|^2 \dots |\phi_N(\bar{\mathbf{r}}_{i_N})|^2 \quad (\text{B12})$$

where the summation runs over all possible permutations of the atomic coordinates  $i = (1, \dots, N)$ . Since there are  $N!$  such permutations, we can express the joint probability distribution in terms of the positions of an atom in the  $j$ th lattice site  $\mathbf{r}_j$ , instead of the position coordinates of the  $j$ th atom  $\bar{\mathbf{r}}_j$ . Each  $N!$  term contributes equally in the sum and we obtain for the joint probability distribution of the position of an atom in the lattice sites  $j = (1, \dots, N)$  in the coordinate representation  $(\mathbf{r}_1, \dots, \mathbf{r}_N)$

$$P'(\mathbf{r}_1, \dots, \mathbf{r}_N) \simeq |\phi_1(\mathbf{r}_1)|^2 \dots |\phi_N(\mathbf{r}_N)|^2 \quad (\text{B13})$$

In the resulting joint probability distribution the position coordinates of atoms within each site  $j$  are independent stochastic variables that are sampled from the Gaussian distributions  $\rho_j(\mathbf{r}) = |\phi_j(\mathbf{r})|^2$ , corresponding to the stochastic Monte-Carlo sampling procedure implemented in the previous section.

### Appendix C: The incident light

By exploiting interactions between the atoms, one can tailor the incident field so that it drives specific linear combinations of collective modes, providing a desired collective response. In the text, for example, we consider phase modulated driving that can excite an array of isolated atoms arranged in a checkerboard pattern on an optical lattice. A spatial light modulator is employed to produce an incident field approximately of the form

$$\mathbf{E}_{\text{in}}^+(\mathbf{r}, t) = \hat{\mathbf{e}}_y E_0 e^{i(kz - \Omega t)} e^{i\varphi(x, y)}, \quad (\text{C1})$$

where

$$\varphi(x, y) = \varphi_{\text{max}} \sin(\kappa x) \sin(\kappa y). \quad (\text{C2})$$

A field profile of this form, however, contains evanescent plane wave components whose transverse wavevectors exceed the carrier wave number  $k$ . We therefore approximate this phase modulated field through the truncated Fourier expansion

$$\mathbf{E}_{\text{in}}^+ = \sum_{m, n} C_{m, n} \hat{\mathbf{e}}_{m, n} e^{i(\mathbf{k}_{m, n} \cdot \mathbf{r} - \Omega t)}, \quad (\text{C3})$$

where  $\mathbf{k}_{m, n} = m\kappa\hat{\mathbf{e}}_x + n\kappa\hat{\mathbf{e}}_y + q_{m, n}\hat{\mathbf{e}}_z$ ,  $q_{m, n} \equiv \sqrt{(\Omega/c)^2 - \kappa^2(m^2 + n^2)}$ , and  $\hat{\mathbf{e}}_{m, n}$  is the normalized projection of the vector  $\hat{\mathbf{e}}_y$  onto the plane perpendicular to  $\mathbf{k}_{m, n}$ . We have truncated the expansion for values of  $m$  and  $n$  for which  $q_{m, n}^2 \geq 0$ .

Because our goal was to produce a phase modulated driving of the meta-atoms, we choose  $C_{m, n}$  so as to reproduce a phase modulated driving, i.e.

$$\hat{\mathbf{d}} \cdot \mathbf{E}_{\text{in}}^+ = \sum_{m, n} C_{m, n} (\hat{\mathbf{d}} \cdot \hat{\mathbf{e}}_{m, n}) e^{i(\mathbf{k}_{m, n} \cdot \mathbf{r} - \Omega t)} \quad (\text{C4})$$

$$\approx \hat{\mathbf{d}} \cdot \hat{\mathbf{e}}_y e^{i\varphi(x, y)} e^{i(kz - \Omega t)}, \quad (\text{C5})$$

The coefficients  $C_{m, n}$  are obtained from the discrete Fourier transform of the phase modulation  $\exp(i\varphi(x, y))$  and dividing by  $\hat{\mathbf{e}}_{m, n} \cdot \hat{\mathbf{d}}$ .

[1] M. Greiner, O. Mandel, T. Esslinger, T. W. Hänsch, and I. Bloch, *Nature* **415**, 39 (2002).

[2] T. Stöferle, H. Moritz, C. Schori, M. Köhl, and

- T. Esslinger, Phys. Rev. Lett. **92**, 130403 (2004).
- [3] B. Paredes, A. Widera, V. Murg, O. Mandel, S. Fölling, I. Cirac, G. V. Shlyapnikov, T. W. Hänsch, and I. Bloch, Nature **429**, 277 (2004).
- [4] R. Jördens, N. Strohmaier, K. Günter, H. Moritz, and T. Esslinger, Nature **455**, 204 (2008).
- [5] U. Schneider, L. Hackermüller, S. Will, T. Best, I. Bloch, T. A. Costi, R. W. Helmes, D. Rasch, and A. Rosch, **322**, 1520 (2008).
- [6] J. K. Chin, D. E. Miller, Y. Liu, C. Stan, W. Setiawan, C. Sanner, K. Xu, and W. Ketterle, Nature **443**, 961 (2006).
- [7] O. Mandel, M. Greiner, A. Widera, T. Rom, T. W. Hänsch, and I. Bloch, Nature **425**, 937 (2003).
- [8] J. Estève, C. Gross, A. Weller, S. Giovanazzi, and M. K. Oberthaler, Nature **455**, 1216 (2008).
- [9] C. Weitenberg, M. Endres, J. F. Sherson, M. Cheneau, P. Schauß, T. Fukuhara, I. Bloch, and S. Kuhr, Nature **471**, 319 (2011).
- [10] M. I. Stockman, S. V. Faleev, and D. J. Bergman, Phys. Rev. Lett. **88**, 067402 (2002).
- [11] M. Aeschlimann, M. Bauer, D. Bayer, T. Brixner, S. Cunovic, F. Dimler, A. Fischer, W. Pfeiffer, M. Rohmer, C. Schneider, et al., Proceedings of the National Academy of Sciences **107**, 5329 (2010).
- [12] A. Sentenac and P. C. Chaumet, Phys. Rev. Lett. **101**, 013901 (2008).
- [13] T. S. Kao, S. D. Jenkins, J. Ruostekoski, and N. I. Zheludev, Phys. Rev. Lett. **106**, 085501 (2011).
- [14] A. Lagendijk and B. A. v. Tiggelen, Physics Reports **270**, 143 (1996).
- [15] O. Morice, Y. Castin, and J. Dalibard, Phys. Rev. A **51**, 3896 (1995).
- [16] J. Ruostekoski and J. Javanainen, Phys. Rev. A **55**, 513 (1997).
- [17] J. Ruostekoski and J. Javanainen, Phys. Rev. A **56**, 2056 (1997).
- [18] B. van Tiggelen, in *Diffuse Waves In Complex Media*, edited by Fouque, JP, NATO, Sci Comm (Springer, Dordrecht, Netherlands, 1999), vol. 531 of *NATO Advanced Science Institutes Series, Series C, Mathematical And Physical Sciences*, pp. 1–60.
- [19] J. Javanainen and J. Ruostekoski, Phys. Rev. Lett. **91**, 150404 (2003).
- [20] I. B. Mekhov, C. Maschler, and H. Ritsch, Phys. Rev. Lett. **98**, 100402 (2007).
- [21] J. Ruostekoski, C. J. Foot, and A. B. Deb, Phys. Rev. Lett. **103**, 170404 (2009).
- [22] S. Rist, C. Menotti, and G. Morigi, Phys. Rev. A **81**, 013404 (2010).
- [23] T. A. Corcovilos, S. K. Baur, J. M. Hitchcock, E. J. Mueller, and R. G. Hulet, Phys. Rev. A **81**, 013415 (2010).
- [24] J. S. Douglas and K. Burnett, Phys. Rev. A **84**, 033637 (2011).
- [25] J. S. Douglas and K. Burnett, Phys. Rev. A **84**, 053608 (2011).
- [26] M. Antezza and Y. Castin, Phys. Rev. Lett. **103**, 123903 (2009).
- [27] O. Morsch and M. Oberthaler, Rev. Mod. Phys. **78**, 179 (2006).
- [28] J. D. Jackson, *Classical Electrodynamics* (John Wiley & Sons, New York, 1998).
- [29] J. Javanainen, J. Ruostekoski, B. Vestergaard, and M. R. Francis, Phys. Rev. A **59**, 649 (1999).
- [30] L. Chomaz, L. Corman, T. Yefsah, R. Desbuquois, and J. Dalibard, arXiv:1112.3170 (2011).
- [31] S. Al-Assam, R. A. Williams, and C. Foot, Phys. Rev. A **82**, 021604 (2010).
- [32] M. Shotton, D. Trypogeorgos, and C. Foot, Phys. Rev. A **78**, 051602 (2008).